Title
Cochannel Receivers for CPM signals Based Upon the Laurent Representation

Authors
Murphy, P. A.
Ford, Gary

Publication Date
1996

Peer reviewed

Cochannel Receivers for CPM Signals Based Upon the Laurent Representation

Peter A. Murphy & Gary E. Ford

CIPIC, Center for Image Processing and Integrated Computing
University of California, Davis, CA 95616
e mail: murphy@ece.ucdavis.edu, ford@ece.ucdavis.edu
Tel: (916)752-2387, Fax: (916)752-8894

Abstract

In this paper, we develop optimum and suboptimum receivers for jointly detecting two cochannel continuous phase modulated (CPM) signals. These receivers are based upon Laurent's representation of binary CPM as the sum of a finite number of pulse amplitude modulated signals. We also provide a review of the Laurent representation and its application to the design of optimum and suboptimum single-channel receivers.

1 Introduction

Cochannel interference, which occurs when two or more signals share the same spectral and temporal channels, is a major obstacle to high quality speech and data transmission in mobile radio systems [1, 2]. In a recent paper [3], we investigated a single-sensor technique for jointly detecting two cochannel CPM signals. The result was the development of the joint maximum likelihood sequence estimation (JMLSE) receiver based upon the conventional representation of CPM [4]. It was shown that this receiver performed well under certain conditions even when the power separation between the signals was negligible. One of the major drawbacks with this receiver, however, is its high degree of complexity.

In an effort to simplify the receiver and provide new perspectives on the joint detector, we have investigated the use of the Laurent representation [5] for binary CPM in developing both optimum and suboptimum cochannel receivers. In [5], Laurent showed that a binary CPM signal can be exactly represented as the sum of K pulse amplitude modulated (PAM) signals. The Laurent representation is a generalization of the interpretation of MSK-type signals (i.e., binary CPM with modulation index 1/2) as the sum of time and phase shifted PAM signals [6, 7]. For example, it is well known that MSK can be represented as an offset-QPSK signal in which the pulse shape is a half-cycle sinusoid with period four times the bit duration. There are three main advantages of the Laurent representation. First, it provides for easy calculation of the autocorrelation and power spectrum of CPM signals. Second, it provides for easy inclusion of channel effects in the expression for an LTI-filtered CPM signal. Third, and more important to the discussion in this paper, it provides a straightforward method of accurately approximating CPM signals using only a subset of the K PAM components in the exact representation.

A number of researchers have found the Laurent representation useful [8, 9, 10, 11, 12, 13, 14, 15, 16, 17, 18]. In [8], Kaleh employed the representation to develop the optimum maximum likelihood sequence estimation (MLSE) receiver for a single CPM signal in additive white Gaussian noise. It was pointed out that this optimum receiver has the same complexity as the MLSE receiver developed based upon the conventional representation of CPM [4]. The author also developed suboptimum receivers by approximating the CPM signals using a subset of the K PAM components in the Laurent representation. In Section 3, we will rely heavily on much of Kaleh's work.

Many researchers have used only the primary PAM component of the Laurent representation to develop simplified receivers. Baier [9] showed that when MSK-type signals are approximated using the primary component, a *derotation* technique simplifies the receiver design. Luise and Mengali [10] illustrated that for MSK-type signals, the average matched filter (AMF) [4, 19] used as the receive filter in a linear MSK-type receiver, is simply the time-reversed version of the primary pulse in the Laurent representation. In [11], Kaleh

developed a differential detector for MSK-type signals and showed that the structure of the receiver is similar to a differential detector for BPSK, except that unlike a conventional differential detector, which multiplies two signals one of which is delayed by the symbol period T, a longer delay MT provides a performance improvement over a delay T. Del Re et al. [12, 13] developed a simplified receiver for a filtered normal burst in the GSM system. In [16], the authors describe a simplified Viterbi processor for the demodulation of the GMSK bursts used in the GSM system. The authors approximated the differentially encoded GMSK signal using the primary PAM component in the Laurent representation. In [17] the authors develop a noncoherent receiver for the GMSK signals used in the Digital European Cordless Telecommunications (DECT) system. Once again, the receiver is based upon approximating the CPM signals using the primary pulse of the Laurent representation.

The approach taken in this paper to develop optimum and suboptimum ML receivers for jointly detecting two cochannel CPM signals is based upon the Laurent representation. The paper is somewhat tutorial in nature, simply because the development of the joint detectors requires the necessary background material provided in the early part of this paper. Furthermore, these early sections include examples of the material applied to MSK signals and the GMSK signals used the European GSM [20] and DCS1800 [21] systems.

The structure of the paper is as follows. In Section 2 we review the Laurent representation for binary CPM signaling. Following this, Section 3 provides a discussion of optimum and suboptimum ML receivers for CPM signals based upon the Laurent representation and its approximation. This section, although primarily a review, does include some new results on the performance of suboptimum receivers applied to GMSK signaling. In particular, we show that for the GMSK signals used in the GSM and DCS1800 systems, a reduction in complexity by a factor of four is attainable with only a slight degradation in receiver performance relative to the optimum receiver. Next, Section 4 describes both optimum and suboptimum receivers for jointly detecting cochannel CPM signals. Once again, we illustrate that use of the Laurent approximation reduces the receiver complexity by a factor of four relative to the optimum joint detector. Finally, the paper provides some concluding remarks in Section 5.

2 Laurent's Representation

A binary CPM signal can be expressed as [4]

$$s(t) = Re[s_b(t,\underline{\alpha})e^{j\,2\pi f_c t}] \quad t \geq 0 \tag{1}$$

$$s_b(t,\underline{\alpha}) = \sqrt{\frac{2E_b}{T}}e^{j[\theta(t)+\phi]} \quad t \geq 0 \tag{2}$$

$$\theta(t) = 2\pi h \int_0^t \sum_{i=0}^{N-1} \alpha_i g(\tau - iT)d\tau \quad t \geq 0 \tag{3}$$

$$= \pi h \sum_{i=0}^{N-1} \alpha_i q(t - iT) \quad t \geq 0, \tag{4}$$

where f_c is the carrier frequency, ϕ is the carrier phase, which for the remainder of this section is assumed to be zero, E_b is the energy per bit, T is the bit period, h is the modulation index which takes on rational values (i.e., $h = 2k/p$ k,p integers), $\{\alpha_i\}$ are the transmitted bits taken from the set $\{-1,1\}$ with equal probability, $g(t)$ is termed the frequency pulse and is nonzero in the interval $[0,LT]$, has area equal to $1/2$ and is symmetric about $LT/2.$, and $q(t)$ is the integral of the frequency pulse, such that

$$q(t) = \int_0^t g(\tau)d\tau \tag{5}$$

$$q(LT) = 1/2. \tag{6}$$

As Laurent [5] showed, the complex baseband signal $s_b(t,\underline{\alpha})$ can be expressed as the sum of $K = 2^{L-1}$ PAM signals, i.e.,

$$s_b(t,\underline{\alpha}) = \sqrt{\frac{2E_b}{T}} \sum_{k=0}^{K-1} \sum_{n=0}^{N-1} [e^{j\pi h a_{k,n}}] c_k(t - nT) \tag{7}$$

over the interval $t \in [LT, NT]$, where

$$\begin{aligned} a_{k,n} &= \sum_{i=o}^{n} \alpha_i - \sum_{j=1}^{L-1} \alpha_{n-j}\beta_{k,j} \\ &= a_{o,n} - \sum_{j=1}^{L-1} \alpha_{n-j}\beta_{k,j}, \\ &= a_{o,n-L} + \sum_{j=1}^{L-1} \alpha_{n-j}(1-\beta_{k,j}) + \alpha_n, \end{aligned} \tag{8}$$

where the set $\{\beta_{k,j}\}$ are used in the binary representation of the index k:

$$k = \sum_{j=1}^{L-1} 2^{j-1}\beta_{k,j} \quad k \in [0, K-1] \tag{9}$$

and $\beta_{k,j} \in \{0, 1\}$. Finally, the functions of time $c_k(t)$ are are given by

$$c_k(t) = s_0(t) \prod_{j=1}^{L-1} s_{j+L\beta k,j}(t) \quad k \in [0, K-1], \tag{10}$$

where

$$s_j(t) = \frac{sin(\Psi(t+jT))}{sin(\pi h)} = s_0(t+jT), \tag{11}$$

$$\Psi(t) = \begin{cases} \phi(t) & t \in [0, LT) \\ \pi h - \phi(t-LT) & t \in [LT, 2LT] \\ 0 & else \end{cases}$$

and

$$\phi(t) = 2\pi h \int_0^t g(\tau)d\tau \tag{12}$$

Example 2.1 The Laurent Representation for MSK
In this example, we present the Laurent representation for MSK. Recall, for MSK $L = 1$, $h = 1/2$, and

$$g(t) = \begin{cases} \frac{1}{2T}, & t \in [0, T] \\ 0, & \text{otherwise} \end{cases}$$

Therefore, we have $K = 2^{L-1} = 1$, so that the Laurent representation of (7) includes only one function of time $c_0(t)$. It can be shown that

$$c_0(t) = \begin{cases} \sin(\frac{\pi t}{2T}), & t \in [0, 2T) \\ 0, & \text{otherwise} \end{cases}$$

This provides the well known interpretation of MSK as offset-QPSK in which the pulse shape is a half-cycle sinusoid with period $4T$. The complex, baseband representation for MSK is given by

$$s_b(t, \underline{\alpha}) = \sqrt{\frac{2E_b}{T}} \sum_{n=0}^{N-1} [e^{j\frac{\pi}{2}a_{0,n}}] c_0(t-nT) \tag{13}$$

Example 2.2 The Laurent Representation for GMSK
In this example, we present the Laurent representation for the GMSK signals used in the European GSM and DCS1800 systems. In particular, the GMSK signal parameters are $BT = 0.3$, $L = 3$, and $h = 1/2$. We see that $K = 2^{L-1} = 4$, so that we have four signals components $c_0(t)$, $c_1(t)$, $c_2(t)$, and $c_3(t)$, as shown in Figure 1. The phase variables $\{a_{k,n},\ k \in [0, 3]\}$ are given by

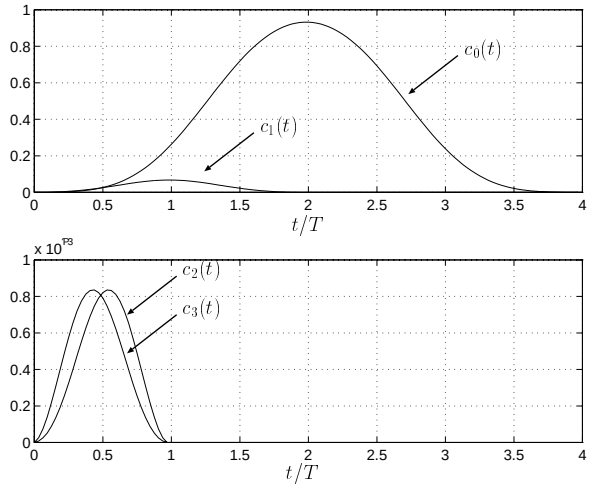

Figure 1: Signal components of GMSK with $L = 3$, $BT = 0.3$, and $h = 1/2$

$$a_{0,n} = \sum_{i=0}^{n-3} \alpha_i + \alpha_{n-2} + \alpha_{n-1} + \alpha_n \tag{14}$$

$$a_{1,n} = \sum_{i=0}^{n-3} \alpha_i + \alpha_{n-2} + \alpha_n \tag{15}$$

$$a_{2,n} = \sum_{i=0}^{n-3} \alpha_i + \alpha_{n-1} + \alpha_n \tag{16}$$

$$a_{3,n} = \sum_{i=0}^{n-3} \alpha_i + \alpha_n \tag{17}$$

The Laurent representation for this signal is given by

$$s_b(t, \underline{\alpha}) = \sqrt{\frac{2E_b}{T}} \sum_{k=0}^{3} \sum_{n=0}^{N-1} [e^{j\frac{\pi}{2}a_{k,n}}] c_k(t - nT) \tag{18}$$

We should highlight that the $c_0(t)$ signal component in general provides most of the signal energy for all CPM signals. For the GMSK signals described above, computer simulations reveal that 99.7236% of the signal energy is contained in the $c_0(t)$ component, $c_1(t)$ contains 0.2763% of the signal energy, and the remaining signal energy is shared between the $c_2(t)$ and $c_3(t)$ components.

---

3 Single-channel Receivers Based Upon Laurent's Representation

In this section, we develop coherent optimum and suboptimum demodulators for a single CPM signal based upon the Laurent representation. We should highlight that much of this section is a review of theory developed by Kaleh [8]. However, the performance results presented in Examples 3.1 and 3.2 are new. Section 3.1 includes a description of the optimum maximum likelihood sequence estimation (MLSE) receiver for CPM signals corrupted by additive white Gaussian noise (AWGN). Section 3.2 includes a description of less complex, suboptimum receivers for these same received signals based upon approximating the signals using a subset of the K PAM components in the Laurent representation.

3.1 Optimum ML Receiver for CPM Signals in AWGN

The signal to be processed in the coherent receiver is

$$r(t) = s_b(t, \underline{\alpha}) + n(t), \ t \in [LT, NT] \tag{19}$$

where $n(t)$ is a realization of a complex, zero mean, white Gaussian noise process. The ML receiver maximizes the log likelihood function [22]

$$ln[P_{r(t)|\underline{\hat{\alpha}}}(r(t)|\underline{\hat{\alpha}})] \propto -\int_{LT}^{NT} |r(t) - s_b(t, \underline{\hat{\alpha}})|^2 dt \tag{20}$$

with respect to the estimated sequence $\underline{\hat{\alpha}} = [\hat{\alpha}_L, \hat{\alpha}_{L+1}, \cdots, \hat{\alpha}_{N-1}]$, where we assume knowledge of $[\alpha_0, \alpha_1, \cdots, \alpha_{L-1}]$. This receiver criterion can be simplified to choose the $\underline{\hat{\alpha}}$ that maximizes the metric

$$\Lambda(\underline{\hat{\alpha}}) = \int_{LT}^{NT} Re\{r(t)s_b^*(t, \underline{\hat{\alpha}})\} dt \tag{21}$$

where $Re(\cdot)$ denotes the real part of $(\cdot)$ and $(\cdot)^*$ denotes the complex conjugate of $(\cdot)$. Substituting (7) into (21) yields

$$\begin{aligned} \Lambda(\underline{\hat{\alpha}}) &= \sqrt{\frac{2E_b}{T}} \int_{LT}^{NT} Re\left\{ r(t) \left[\sum_{k=0}^{K-1} \sum_{n=0}^{N-1} e^{j\pi h \hat{a}_{k,n}} c_k(t - nT) \right]^* \right\} dt \\ &= \sqrt{\frac{2E_b}{T}} \sum_{n=0}^{N-1} Re\{\lambda(n)\}, \end{aligned} \tag{22}$$

where

$$\lambda(n) = \sum_{k=0}^{K-1} r_{k,n} e^{-j\pi h \hat{a}_{k,n}} \tag{23}$$

where the $\{\hat{a}_{k,n}\}$ are calculated using (8) with $\{\alpha_i\}$ replaced by $\{\hat{\alpha}_i\}$ and

$$r_{k,n} = [r(t) * c_k^*(-t)]|_{t=nT} = \int r(t) c_k^*(t - nT) dt \tag{24}$$

The samples $\{r_{k,n}\}$ form a set of sufficient statistics for the computation of $\Lambda(\underline{\hat{\alpha}})$. Furthermore, (24) shows that they can be acquired by sampling at times nT the output of K matched filters $\{c_k^*(-t),\ k \in [0, K-1]\}$ fed by the received signal $r(t)$. From Section 2, we know that the pulses $\{c_k(t),\ k \in [0, K-1]\}$ are real-valued and therefore the conjugation of $c_k(-t)$ in (24) is not necessary. However, we include the conjugation operation, because it provides for an easy extension of the algorithm to handle the effects of a possibly complex-valued LTI channel impulse response. The calculation of $\lambda(n)$ at time nT, requires knowledge of all possible $\{\hat{a}_{k,n},\ k \in [0, K-1]\}$, which in turn depend upon the phase state $\pi h \hat{a}_{0,n-L}$, the state vector $[\hat{\alpha}_{n-1}, \hat{\alpha}_{n-2}, \cdots, \hat{\alpha}_{n-L+1}]$, and the symbol $\hat{\alpha}_n$. For $h = 2i/p$ (i, p integers), $\pi h \hat{a}_{0,n-L}$ takes on p discrete values $\{0, 2\pi/p, \cdots, 2\pi(p-1)/p\}$. It is easily shown that at each time nT, the maximum likelihood receiver computes $\lambda(n)$ for all possible 2^L sequences $[\hat{\alpha}_n, \hat{\alpha}_{n-1}, \cdots, \hat{\alpha}_{n-L+1}]$ and all p possible phase states $\pi h \hat{a}_{0,n-L}$. Therefore, there are $p2^L$ metrics calculated per symbol interval. As one might expect, this is the same number calculated by the MSLE receiver based upon the conventional representation of CPM [4]. The computationally efficient Viterbi algorithm can be employed to choose the sequence $\underline{\hat{\alpha}}$ that maximizes $\Lambda(\underline{\hat{\alpha}})$. Figure 2 shows the structure of the receiver. The constant $\sqrt{2E_b/T}$ in (22) is not necessary and can be omitted. However, we include it here because the joint detector of Section 4 requires it.

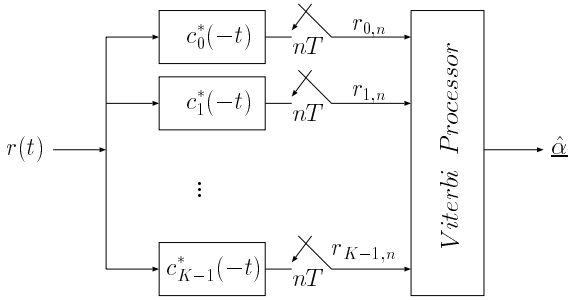

Figure 2: Optimum MLSE Receiver for binary CPM based upon Laurent's Representation

Example 3.1 The MLSE Receiver for MSK Signaling

In this example, we briefly describe the MLSE receiver for MSK. Recall, that in Example 2.1, we developed the Laurent representation for MSK and explained that for this signal, $K = 1$. The ML receiver chooses the sequence $\underline{\hat{\alpha}}$ that maximizes (22), where

$$\lambda(n) = r_{0,n} e^{-j\frac{\pi}{2}\hat{a}_{0,n}} \tag{25}$$

$$r_{0,n} = [r(t) * c_0^*(-t)]|_{t=nT} = \int r(t) c_0^*(t - nT) dt \tag{26}$$

The samples $\{r_{0,n}\}$ are obtained by sampling at times nT the output of the matched filter $c_0^*(-t)$ fed by the received signal $r(t)$. The calculation of $\lambda(n)$ at time nT requires knowledge of the phase state $\frac{\pi}{2}\hat{a}_{0,n-1}$ and the symbol $\hat{\alpha}_n$. It is easily shown that $\frac{\pi}{2}\hat{a}_{0,n-1}$ takes on 4 possible values $\{0, \pi/2, \pi, 3\pi/2\}$ and $\hat{\alpha}_n$ takes on 2 possible values. Therefore, during each symbol interval $8 = 2 \cdot 4$ metrics are calculated.

Example 3.2 The MLSE Receiver for GMSK Signaling

In this example, we develop the optimum receiver for the GMSK signals described in Example 2.2. The Laurent representation for this signal consists of the four signal components $c_0(t)$, $c_1(t)$, $c_2(t)$, and $c_3(t)$ shown in Figure 1. The phase variables $\{a_{k,n}, k \in [0, K-1]\}$ are given by equations (14)-(17). It can be shown that this receiver requires the calculation of $32 = p2^L$ metrics per symbol interval. The receiver structure is shown in Figure 3. Figure 4 illustrates the performance of this receiver in terms of bit-error-rate (BER) relative to the more conventional MLSE receiver [4]. The BER curves are calculated via computer simulations. We can see that the performance of the Laurent-based MLSE receiver developed in this section is identical to the conventional MLSE receiver, which is no surprise since the Laurent representation is an exact representation and since both receivers attempt to maximize the same likelihood function. The plot also includes the performance of the reduced complexity receiver described in Example 3.3.

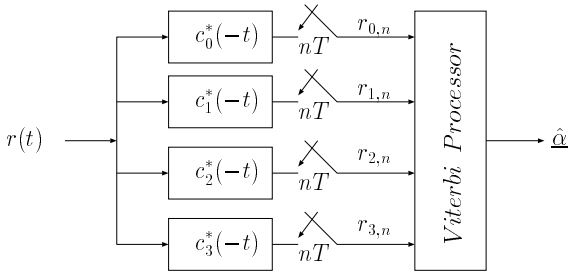

Figure 3: Optimum MLSE Receiver for GMSK Signals

3.2 Suboptimum Receivers for CPM Signals in AWGN

Less complex, suboptimum receivers can be developed for CPM by approximating the signals using a subset of the K PAM components in the Laurent representation (see (7)). Though suboptimum, these receivers admit only a slight degradation in performance relative to the optimum receiver. The suboptimum receiver is developed by first approximating the CPM signal using the first $\tilde{K}$ components, where $\tilde{K} \leq K$, of the Laurent representation, i.e.,

$$\tilde{s}_b(t, \underline{\alpha}) = \sqrt{\frac{2E_b}{T}} \sum_{k=0}^{\tilde{K}-1} \sum_{n=0}^{N-1} [e^{j\pi h a_{k,n}}] c_k(t - nT) \tag{27}$$

where the $\{a_{k,n}, k \in [0, \tilde{K}-1]\}$ are calculated using (8). When $\tilde{K} = K$, the approximation in (27) is equal to the exact representation of (7), and the suboptimum receiver becomes the optimum ML receiver of Section 3.1.

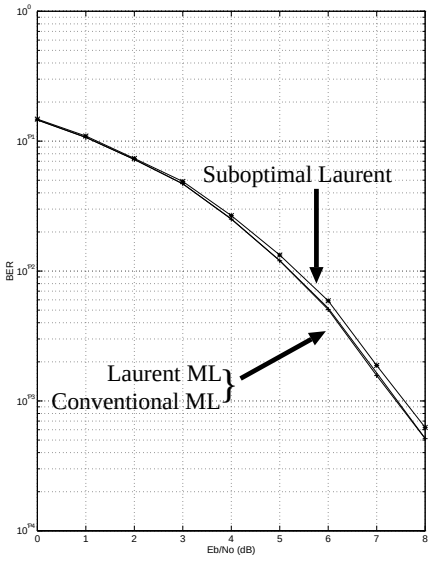

Figure 4: BER for conventional, Laurent, and suboptimum MLSE receivers

Following a procedure similar to that of Section 3.1, let the approximate received signal be given by

$$r(t) = \tilde{s}_b(t, \underline{\alpha}) + n(t), \ t \in [LT, NT] \tag{28}$$

where $n(t)$ is a realization of a complex, zero mean, white Gaussian noise process. Once again, the ML receiver maximizes the log likelihood function

$$ln[P_{r(t)}|\underline{\hat{\alpha}}(r(t)|\underline{\hat{\alpha}})] \propto -\int_{LT}^{NT} |r(t) - \tilde{s}_b(t, \underline{\hat{\alpha}})|^2 dt \tag{29}$$

with respect to the estimated sequence $\underline{\hat{\alpha}} = [\hat{\alpha}_L, \hat{\alpha}_{L+1}, \cdots, \hat{\alpha}_{N-1}]$, where we assume knowledge of $[\alpha_0, \alpha_1, \cdots, \alpha_{L-1}]$. Of course, this receiver is not optimum because $\tilde{s}_b(t, \underline{\hat{\alpha}})$ is an approximation. This receiver criterion can be simplified to choose the $\underline{\hat{\alpha}}$ that maximizes the metric

$$\tilde{\Lambda}(\underline{\hat{\alpha}}) = \int_{LT}^{NT} Re\{r(t)\tilde{s}_b^*(t, \underline{\hat{\alpha}})\} dt \tag{30}$$

Substituting (27) into (30) yields

$$\tilde{\Lambda}(\underline{\hat{\alpha}}) = \sqrt{\frac{2E_b}{T}} \sum_{n=0}^{N-1} Re\{\tilde{\lambda}(n)\}, \tag{31}$$

where

$$\tilde{\lambda}(n) = \sum_{k=0}^{\tilde{K}-1} r_{k,n} e^{-j\,\pi h\,\hat{a}_{k,n}} \tag{32}$$

$$r_{k,n} = [r(t) * c_k^*(-t)]|_{t=nT} = \int r(t) c_k^*(t - nT) dt \tag{33}$$

Once again, the samples $\{r_{k,n}\}$ can be obtained by sampling at times nT the output of the $\tilde{K}$ matched filters $\{c_k^*(-t), k \in [0, \tilde{K}-1]\}$ simultaneously fed by the received signal $r(t)$. The calculation of $\tilde{\lambda}(n)$ at time nT requires the knowledge of all possible $\{\hat{a}_{k,n}, \ k \in [0, \tilde{K}-1]\}$. We should highlight that in this case, the phase state is given by $\pi h \hat{a}_{0,n-L+i}$. The value of i is dependent upon the $\{\beta_{k,j}\}$ of (9) used in the binary representation of k. It can be shown that at each time nT, this suboptimum receiver computes $\tilde{\lambda}(n)$ for all possible 2^{L-i} sequences $[\hat{\alpha}_n, \hat{\alpha}_{n-1}, \cdots, \hat{\alpha}_{n-L+1+i}]$ and all p possible phase states $\pi h \hat{a}_{0,n-L+i}$. Thus, there are $p2^{L-i}$ metrics calculated per symbol interval. Recall from Section 3.1, the optimum receiver requires the calculation of $p2^L$ metrics. Therefore, this receiver provides a reduction in complexity by a factor of 2^i.

Moreover, the receiver requires $\tilde{K}$ matched filters instead of the K matched filters required in the optimum receiver.

Example 3.3 Suboptimum Receiver for GMSK Signaling

In this example, we develop a suboptimum receiver for the GMSK signals in Examples 2.2 and 3.2. We approximate the GMSK signals using only the primary component $c_0(t)$ and develop the ML receiver based on this approximation. As stated in Example 2.2, the portion of the GMSK signal due to the $c_0(t)$ component contains over 99% of the signal energy, and is, therefore, a very good approximation. The GMSK signal is approximated as

$$\tilde{s}_b(t, \underline{\alpha}) = \sqrt{\frac{2E_b}{T}} \sum_{n=0}^{N-1} [e^{j\frac{\pi}{2}a_{0,n}}] c_0(t - nT) \tag{34}$$

Using the results presented earlier in this section, the suboptimum ML receiver maximizes the metric $\tilde{\Lambda}(\underline{\hat{\alpha}})$, given by (31) with

$$\tilde{\lambda}(n) = r_{0,n} e^{-j\frac{\pi}{2}\hat{a}_{0,n}}, \tag{35}$$

where $r_{0,n}$ is the output of the matched filter $c_0^*(-t)$ sampled at times nT whose input is the received signal $r(t)$. Using the results from Example 2.2, we know

$$\hat{a}_{0,n} = \hat{\alpha}_n + \sum_{i=0}^{n-1} \hat{\alpha}_i \tag{36}$$

The calculation of $\tilde{\lambda}(n)$ at time nT requires knowledge of the phase state $\frac{\pi}{2}\hat{a}_{0,n-1}$ and $\hat{\alpha}_n$. It can be shown that this suboptimum receiver computes $\tilde{\lambda}(n)$ for the 2 possible values of $\hat{\alpha}_n$ and all 4 possible values of the phase state. Therefore, there are 8 metrics calculated per symbol interval. Recall, the optimum ML receiver for GMSK developed in Example 3.2, required the calculation of 32 metrics per symbol interval. Therefore, this simplified receiver reduces complexity by a factor of 4. Figure 4 illustrates the BER performance of the simplified receiver. The plot reveals that the suboptimum receiver admits only a slight degradation in performance relative to the optimum receiver. Furthermore, this example highlights that by approximating a CPM signal with modulation index 1/2 using the primary PAM component of the Laurent representation, the suboptimum receiver has the same complexity as the optimum MLSE receiver for MSK (see Example 3.1). That is, the receiver requires the calculation of only 8 metrics per symbol interval.

---

4 Cochannel Receivers Based Upon Laurent's Representation

In this section, we develop novel optimum and suboptimum demodulators for jointly detecting two cochannel CPM signals. The receivers are based upon the Laurent representation described in Section 2. Section 4.1 includes a description of the optimum joint maximum likelihood sequence estimation (JMLSE) receiver and Section 4.2 includes a description of less complex, suboptimum receivers for these same signals.

4.1 Optimum ML Receiver for Cochannel CPM Signals in AWGN

The signal to be processed by the coherent receiver is the sum of two complex baseband CPM signals and complex white Gaussian noise. The received signal can be expressed as

$$r(t) = s_{b,1}(t, \underline{\alpha}_1) + s_{b,2}(t, \underline{\alpha}_2) + n(t), \; t \in [LT, NT] \tag{37}$$

where

$$s_{b,1}(t, \underline{\alpha}_1) = \sqrt{\frac{2E_{b,1}}{T}} e^{j[\theta_1(t)+\phi_1]} \quad t \geq 0 \tag{38}$$

$$s_{b,2}(t, \underline{\alpha}_2) = \sqrt{\frac{2E_{b,2}}{T}} e^{j[\theta_2(t)+\phi_2]} \quad t \geq 0 \tag{39}$$

We should highlight that even though the two CPM signals are similar in structure, they may have different modulation indices h_1 and h_2, different energy levels $E_{b,1}$ and $E_{b,2}$, different carrier phases ϕ_1 and ϕ_2,

different frequency pulses $g_1(t)$ and $g_2(t)$, each with its own length of temporal support L_1 and L_2, and of course the transmitted bit sequences $\underline{\alpha}_1$ and $\underline{\alpha}_2$ are distinct. However, we do assume the signals share the same bit period T and that both signals transmit an equal number of bits N . Finally, L is chosen as the maximum value of L_1 and L_2.

The joint maximum likelihood receiver maximizes the log likelihood function

$$\ln\left[P_{r(t)|\underline{\hat{\alpha}}_1,\underline{\hat{\alpha}}_2}(r(t)|\underline{\hat{\alpha}}_1,\underline{\hat{\alpha}}_2)\right] \propto -\int_{LT}^{NT} |r(t) - s_{b,1}(t,\underline{\hat{\alpha}}_1) - s_{b,2}(t,\underline{\hat{\alpha}}_2)|^2 dt \tag{40}$$

with respect to the estimated sequences $\underline{\hat{\alpha}}_1 = [\hat{\alpha}_{1,L}, \hat{\alpha}_{1,L+1}, \cdots, \hat{\alpha}_{1,N}]$ and $\underline{\hat{\alpha}}_2 = [\hat{\alpha}_{2,L}, \hat{\alpha}_{2,L+1}, \cdots, \hat{\alpha}_{2,N}]$, where we assume knowledge of $[\alpha_{1,0}, \alpha_{1,1}, \cdots, \alpha_{1,L-1}]$ and $[\alpha_{2,0}, \alpha_{2,1}, \cdots, \alpha_{2,L-1}]$. The above maximization can be simplified to choose the $\underline{\hat{\alpha}}_1$ and $\underline{\hat{\alpha}}_2$ that maximize the metric

$$\Lambda(\underline{\hat{\alpha}}_1,\underline{\hat{\alpha}}_2) = \int_{LT}^{NT} Re\{r(t)s^*_{b,1}(t,\underline{\hat{\alpha}}_1) + r(t)s^*_{b,2}(t,\underline{\hat{\alpha}}_2) - s_{b,1}(t,\underline{\hat{\alpha}}_1)s^*_{b,2}(t,\underline{\hat{\alpha}}_2)\}dt \tag{41}$$

Viewing (41), we see that the first two terms are basically the classic correlation receivers for detecting $\underline{\alpha}_1/\underline{\alpha}_2$ when $s_{b,2}(t,\underline{\alpha}_2)/s_{b,1}(t,\underline{\alpha}_1)$ is not present. The third term tries to ensure that the two signal estimates are uncorrelated.

Using the notation introduced in Section 3.1, substitution of (7) into (41) yields

$$\begin{aligned}\Lambda(\underline{\hat{\alpha}}_1,\underline{\hat{\alpha}}_2) \quad = \quad & \sqrt{\frac{2E_{b_1}}{T}}\sum_{n=0}^{N-1} Re\{\lambda_1(n)\} + \sqrt{\frac{2E_{b_2}}{T}}\sum_{n=0}^{N-1} Re\{\lambda_2(n)\} - \\ & \frac{2}{T}\sqrt{E_{b_1}E_{b_2}}\sum_{n_1=0}^{N-1}\sum_{n_2=0}^{n}\sum_{k_1=0}^{K_1-1}\sum_{k_2=0}^{K_2-1} Re\{e^{j(\pi h_1 \hat{a}^{(1)}_{k_1,n_1} - \pi h_2 \hat{a}^{(2)}_{k_2,n_2} + \phi_1 - \phi_2)} \times \\ & \int_{LT}^{NT} c_{1,k_1}(t-n_1T)c^*_{2,k_2}(t-n_2T)\}dt, \end{aligned} \tag{42}$$

where $\hat{a}^{(1)}_{k,n}$ and $\hat{a}^{(2)}_{k,n}$ are calculated using (8) with $\{\alpha_i\}$ replaced by $\{\hat{\alpha}_{1,i}\}$ and $\{\hat{\alpha}_{2,i}\}$, respectively, and

$$\lambda_1(n) \quad = \quad \sum_{k_1=0}^{K_1-1} r^{(1)}_{k_1,n} e^{-j(\pi h_1 \hat{a}^{(1)}_{k_1,n} + \phi_1)} \tag{43}$$

$$\lambda_2(n) \quad = \quad \sum_{k_2=0}^{K_2-1} r^{(2)}_{k_2,n} e^{-j(\pi h_2 \hat{a}^{(2)}_{k_2,n} + \phi_2)} \tag{44}$$

The samples $r^{(1)}_{k_1,n}$ and $r^{(2)}_{k_2,n}$ are obtained by sampling at times nT the output of the K_1+K_2 matched filters $\{c^*_{1,k_1}(-t),\ k_1 \in [0,K_1-1]\}$ and $\{c^*_{1,k_2}(-t),\ k_2 \in [0,K_2-1]\}$ fed by the received signal $r(t)$. We now turn our attention to the last term in (42). From Section 2, we know

$$c_{1,0}(t) \quad \neq \quad 0,\ t \in [0,(L_1+1)T] \tag{45}$$

$$c_{2,0}(t) \quad \neq \quad 0,\ t \in [0,(L_2+1)T] \tag{46}$$

using this result we can express the last term in (42) as

$$\frac{2}{T}\sqrt{E_{b_1}E_{b_2}}\sum_{n=0}^{N-1}\sum_{n_2=n-L_2}^{n}\sum_{k_1=0}^{K_1-1}\sum_{k_2=0}^{K_2-1} Re\left\{R^{(k_1,k_2)}_{n-n_2} e^{j(\pi h_1 \hat{a}^{(1)}_{k_1,n} - \pi h_2 \hat{a}^{(2)}_{k_2,n_2} + \phi_1 - \phi_2)}\right\} \tag{47}$$

where

$$R^{(k_1,k_2)}_{n-n_2} = \int c_{1,k_1}(t-nT)c^*_{2,k_2}(t-n_2T)dt \tag{48}$$

The terms $R^{(k_1,k_2)}_{n-n_2}$ are a function of the K_1+K_2 PAM components and can be determined in advance and stored in the receiver.

Finally, the optimum receiver chooses the $\underline{\hat{\alpha}}_1$ and $\underline{\hat{\alpha}}_2$ that maximize the metric

$$\Lambda(\underline{\hat{\alpha}}_1, \underline{\hat{\alpha}}_2) = \frac{2}{T}\sqrt{E_{b_1}E_{b_2}}\sum_{n=0}^{N-1} Re[\sqrt{\frac{T}{2E_{b_2}}}\{\lambda_1(n)\} + \sqrt{\frac{T}{2E_{b_1}}}\{\lambda_2(n)\} - \sum_{i=0}^{L_2}\sum_{k_1=0}^{K_1-1}\sum_{k_2=0}^{K_2-1}\left\{R_i^{(k_1,k_2)} e^{j(\pi h_1 \hat{a}^{(1)}_{k_1,n} - \pi h_2 \hat{a}^{(2)}_{k_2,n-i} + \phi_1 - \phi_2)}\right\}] \tag{49}$$

It can be shown that during each symbol interval the receiver requires knowledge of the phase states $\pi h_1 \hat{a}^{(1)}_{0,n-L_1}$ and $\pi h_2 \hat{a}^{(2)}_{0,n-L_2}$, the joint state $[\hat{\alpha}_{1,n-1}, \hat{\alpha}_{1,n-2}, \cdots, \hat{\alpha}_{1,n-L_1+1} \mid \hat{\alpha}_{2,n-1}, \hat{\alpha}_{2,n-2}, \cdots, \hat{\alpha}_{2,n-L_2+1}]$ and the symbols $\hat{\alpha}_{1,n}$ and $\hat{\alpha}_{2,n}$. Therefore, there are $p_1 p_2 2^{L_1+L_2}$ metrics calculated per symbol interval. As one migth expect, this is the same number of metrics required per symbol interval for the JMLSE receiver developed based upon the conventional representation of CPM [3]. Figure 5 illustrates the structure of the optimum cochannel demodulator.

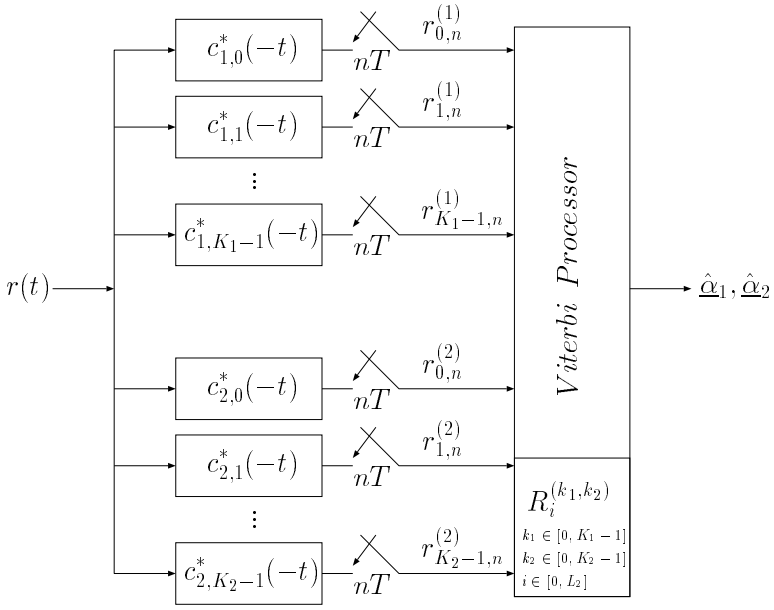

Figure 5: Optimum Cochannel Receiver for binary CPM based upon Laurent's Representation

4.2 Suboptimum ML Receivers for Cochannel CPM Signals in AWGN

In this section, we develop a suboptimum coherent joint maximum likelihood sequence estimation (JMLSE) receiver for jointly detecting two cochannel CPM signals received in additive white Gaussian noise. The approach is similar to that of Section 3.2, except we approximate the two cochannel CPM signals using only the primary PAM component of each signal $c_{1,0}(t)$ and $c_{2,0}(t)$ (refer to (7)).

We let the approximate received be given by

$$r(t) = \tilde{s}_{b,1}(t, \underline{\alpha}_1) + \tilde{s}_{b,2}(t, \underline{\alpha}_2) + n(t), \ t \in [LT, NT], \tag{50}$$

where $\tilde{s}_{b,1}(t, \underline{\hat{\alpha}}_1)$ and $\tilde{s}_{b,2}(t, \underline{\hat{\alpha}}_2)$ are an approximation to the cochannel CPM signals, such that

$$\tilde{s}_{b,1}(t, \underline{\hat{\alpha}}_1) = \sqrt{\frac{2E_{b_1}}{T}}\sum_{n=0}^{N-1} e^{j(\pi h_1 \hat{a}^{(1)}_{0,n} + \phi_1)} c_{1,0}(t - nT) \tag{51}$$

$$\tilde{s}_{b,2}(t, \underline{\hat{\alpha}}_2) = \sqrt{\frac{2E_{b_2}}{T}}\sum_{n=0}^{N-1} e^{j(\pi h_2 \hat{a}^{(2)}_{0,n} + \phi_2)} c_{2,0}(t - nT) \tag{52}$$

It can be shown using results from Section 4.1 that the suboptimum ML receiver chooses the $\underline{\hat{\alpha}}_1$ and $\underline{\hat{\alpha}}_2$ that maximize the metric

$$\begin{aligned}\tilde{\Lambda}(\underline{\hat{\alpha}}_1, \underline{\hat{\alpha}}_2) &= \frac{2}{T}\sqrt{E_{b_1}E_{b_2}}\sum_{n=0}^{N-1}[\sqrt{\frac{T}{2E_{b_2}}}Re\{r_{0,n}^{(1)}e^{-j(\pi h_1 \hat{a}_{0,n}^{(1)}+\phi_1)}\}+ \\ &\sqrt{\frac{T}{2E_{b_1}}}Re\{r_{0,n}^{(2)}e^{-j(\pi h_2 \hat{a}_{0,n}^{(2)}+\phi_2)}\}- \\ &\sum_{i=0}^{L_2} Re\left\{R_i^{(0,0)}e^{j(\pi h_1 \hat{a}_{0,n}^{(1)}-\pi h_2 \hat{a}_{0,n-i}^{(2)}+\phi_1-\phi_2)}\right\}] \end{aligned} \quad (53)$$

We can show that during each symbol interval, this receiver requires knowledge of the phase states $\pi h_1 \hat{a}_{0,n-1}^{(1)}$ and $\pi h_2 \hat{a}_{0,n-L_2}^{(2)}$, the state vector $[\hat{\alpha}_{2,n-1}, \hat{\alpha}_{2,n-2}, \cdots, \hat{\alpha}_{2,n-L_2+1}]$ and the symbols $\hat{\alpha}_{1,n}$ and $\hat{\alpha}_{2,n}$. Therefore, during each symbol interval the receiver requires the calculation of $p_1 p_2 2^{L_2+1}$ metrics. This is a reduction in complexity by a factor of 2^{L_1-1} relative to the optimum detectors of [3] and Section 4.1. Furthermore, as we saw in Section 3.2, this receiver requires only two matched filters $c_{1,0}^*(-t)$ and $c_{2,0}^*(-t)$ compared to the $K_1 + K_2$ required in the optimum receiver.

At the moment no performance results for the suboptimum receiver are available. However, in the future we plan to investigate its performance in detecting cochannel GMSK signals and compare it to the optimum receiver of Section 4.1.

5 Conclusion

In this paper, we employed the Laurent representation to develop optimum and suboptimum joint maximum likelihood sequence estimation (JMLSE) receivers for cochannel CPM signals. In Section 2 we reviewed the Laurent representation and showed that a binary CPM signal can be expressed as the sum of K PAM signals. We also provided examples of how the representation can be used to express MSK signals and the GMSK signals used in the European GSM and DCS1800 systems. Following this, Section 3 included a review of optimum and suboptimum single-channel maximum likelihood receivers for binary CPM signals based upon the Laurent representation. This section also included new performance results highlighting that approximating the GMSK signals in the GSM and DCS1800 systems using only the primary PAM component of the Laurent representation, provided a reduction in receiver complexity by a factor of four, while admitting only a slight degradation in performance. In Section 4 we used the Laurent representation to develop optimum and suboptimum joint maximum likelihood receivers for detecting cochannel CPM signals. We showed that the receiver complexity in the optimum case is equivalent to the complexity of the JMLSE receiver based upon the more conventional representation of CPM. Furthermore, we highlighted that, as in Section 3, the suboptimum receiver provides a factor of four reduction in receiver complexity compared to the optimum joint receiver. In the future, we plan to investigate the performance of the suboptimum joint receiver applied to GMSK signaling. We also plan to examine the use of the Laurent representation to include the effects of channel distortion on single-channel and cochannel CPM signals.

References

[1] D. Cox, "Cochannel interference considerations in frequency reuse small-coverage-area radio systems," *IEEE Trans. Comm.*, vol. COM-30, no. 1, pp. 135–142, Jan. 1982.

[2] S. Wang and S. Rappaport, "Signal-to-interference calculations for balanced channel assignment patterns in cellular communications systems," *IEEE Trans. Comm.*, vol. 37, no. 10, pp. 1077–1087, Oct. 1989.

[3] P. A. Murphy and G. E. Ford, "Cochannel demodulation for continuous phase modulated signals," in *Proc. of the Twenty Eigth Asilomar Conf. on Signals, Systs., and Computers*, 1995.

[4] J. Anderson, T. Aulin, and C. Sundberg, *Digital Phase Modulation.* New York, NY: Plenum Press, 1986.

[5] P. A. Laurent, "Exact and approximate construction of digital phase modulations by superposition of amplitude modulated pulses (AMP)," *IEEE Trans. Comm.*, vol. 34, no. 2, pp. 150 – 160, Feb. 1986.

[6] S. A. Gronemeyer and A. L. McBride, "MSK and offset QPSK modulation," *IEEE Trans. Comm.*, vol. COM-24, no. 8, pp. 809–819, Aug. 1976.

[7] M. K. Simon, "A generalization of minimum-shift-keying (MSK)-type signaling based upon input data symbol pulse shaping," *IEEE Trans. Comm.*, vol. COM-24, no. 8, pp. 845–856, Aug. 1976.

[8] G. K. Kaleh, "Simple coherent receivers for partial response continuous phase modulation," *IEEE J. Select. Areas Comm.*, vol. 7, no. 9, pp. 1427 – 1436, Dec. 1989.

[9] A. Baier, "Derotation techniques in receivers for MSK-type CPM signals," in *Proceedings of the Fifth European Signal Processing Conference (EUSIPCO-90)*, (Barcelona, Spain), pp. 1799–1802, Sept. 1990.

[10] M. Luise and U. Mengali, "A new interpretation of the average matched filter for MSK-type receivers," *IEEE Trans. Comm.*, vol. 39, no. 1, pp. 14 – 16, Jan. 1991.

[11] G. K. Kaleh, "Differentially coherent detection of binary partial response continuous phase modulation with index 0.5," *IEEE Trans. Comm.*, vol. 39, no. 9, pp. 1335 – 1340, Sept. 1991.

[12] E. D. Re, R. Fantacci, L. Pierucci, G. Castellini, and G. Benelli, "Viterbi receiver for mobile radio communications: Issues and implementation remarks," in *Proceedings of the Fifth Tirrenia International Workshop – Coded Modulation and Bandwidth-Efficient Transmission*, (Tirrenia, Italy), pp. 169 – 178, Sept. 1991.

[13] E. D. Re, G. Benelli, G. Castellini, R. Fantacci, L. Pierucci, and L. Pogliani, "Design of a digital mlse receiver for mobile radio communications," in *Proceedings of the IEEE Global Telecommunications Conference (GLOBECOM)*, (Phoenix, AZ), pp. 1469–1473, Dec. 1991.

[14] G. K. Kaleh, "Differential detection via the Viterbi algorithm for offset modulation and MSK-type signals," *IEEE Trans. Vechic. Tech.*, vol. 41, no. 4, pp. 401 – 406, Nov. 1992.

[15] O. Andrisano and M. Chiani, "The first Nyquist criterion applied to coherent receiver design for generalized MSK signals," *IEEE Trans. Comm.*, vol. 42, no. 2/3/4, pp. 449 – 457, Feb/Mar/April 1994.

[16] G. Benelli, A. Garzelli, and F. Salvi, "Simplified Viterbi processors for the GSM pan-European cellular communication system," *IEEE Trans. Vechic. Tech.*, vol. 43, no. 4, pp. 870 – 878, Nov. 1994.

[17] S. Safavi and L. B. Lopes, "A non-coherent equaliser receiver structure for DECT-type systems," in *Proceedings of the 44th Annual Conference of the IEEE Vehicular Technology Society*, (Stockholm, Sweden), pp. 1084 – 1088, June 1994.

[18] A. N. D'Andrea, A. Ginesi, and U. Mengali, "Frequency detectors for CPM signals," *IEEE Trans. Comm.*, vol. 43, no. 2/3/4, pp. 1828 – 1837, February/March/April 1995.

[19] M. S. El-Tanany and S. A. Mahmoud, "Mean-square error optimization of quadrature receivers for CPM with modulation index 1/2," *IEEE J. Select. Areas Comm.*, vol. 5, no. 5, pp. 896 – 905, June 1987.

[20] M. Hodges, "The GSM radio interface," *British Telecom Technology Journal*, vol. 8, no. 1, pp. 31 – 43, Jan. 1990.

[21] P. Ramsdale, "Personal communications in the UK – implementation of PCN using DCS 1800," *Internat. J. Wireless Info. Networks*, vol. 1, no. 1, pp. 29 – 36, Jan. 1994.

[22] J. Proakis, *Digital Communications*. New York: McGraw–Hill, 1989.